Warning: The mini gamma-ray-bursts in planning hadron colliders beyond the LHC energies

Wei Zhu, Zhiyi Cui and Jianhong Ruan
Department of Physics, East China Normal University, Shanghai 200241, China

Abstract

Gluons may converge to a stable state at a critical momentum in nucleon. This gluon condensation will greatly increase the proton-proton cross section provided that the collision energies exceed the gluon condensation threshold. Based on the analyses of cosmic gamma-ray spectra, we find that the $p-Pb$ and $Pb-Pb$ collisions at the LHC are close to the energy region of the gluon condensation effect. We warn that for the next generation of hadron colliders increasing the collision energies, the extremely strong gamma-rays will be emitted in a narrow space of the accelerator due to the gluon condensation effect. Such artificial mini gamma-ray-bursts in the laboratory may damage the detectors.

keywords: Gluon condensation; Gamma-ray-bursts; LHC; LHeC; EIC

1 Introduction

The knowledge of gluon distributions in nucleon are important, since gluons dominate the hadronic processes at high energy. In general, the number of gluons in nucleon grows with gluon splitting. However, this increase of gluons cannot be too fast due to the restriction of the unitarity. The QCD research based on the JIMWLK/BK nonlinear evolution equations predicted that at a critical value of the gluon density, the color-charged gluons may reach an equilibrium state of splitting and fusion, which is called the Color Glass

Condensation (CGC) [1]. An advanced QCD evolution equation proposed by Zhu, Shen and Ruan (ZSR) in [2-3] pointed out that if considering the BFKL singularity in the nonlinear part, the CGC solution will continually evolve to the smaller x range, which will cause the chaotic solution. The dramatic chaotic oscillations will produce strong shadowing and antishadowing effects, forcing the gluons to gather in a state with the critical momentum (x_c, k_c), where x_c is a fraction of proton's longitudinal momentum carried by the condensed gluon and k_c is its transverse momentum (see figure 1). This is the gluon condensation (GC) [4].

The GC will induce significant effect in the nucleon collisions if gluons with the momentum (x_c, k_c) enter the measuring high energy region. Unfortunately, the value of (x_c, k_c) cannot be precisely determined in theory due to the approximations in the derivation of the evolution equation. We have not yet observed the GC-effect in the largest hadron collider– Large Hadron Collider (LHC), which implies that the GC-threshold is beyond the current maximum energies of the LHC. Hence, we turn to consider the collisions of cosmic rays. Protons accelerated in the universe may exceed the GC-threshold and cause the GC-effect in their collisions.

Specifically, cosmic gamma-rays can be generated in hadronic scenario $p + p \to \pi^0 \to 2\gamma$. The sharp peak in the momentum distribution of gluons caused by the GC effect in figure 1 can suddenly increase the cross section in the hadron-hadron collisions, and results in a typical broken power law in the gamma-ray energy spectra, where the break position E_π^{GC} is determined by the critical momentum (x_c, k_c). The broken power law is an often-used parameter formula to describe the very high energy (VHE) gamma-ray spectra. The GC model gives it an intuitive physical explanation. In previous works [5-10] we have used this GC model to explain the VHE gamma-ray spectra originated from supernova remnants (SNRs), active galactic nuclei (AGN), pulsars and gamma-ray-

bursts (GRBs). The knowledge accumulated in these works may help us to improve the prediction ability of the evolution equation.

The purpose of this work is to predict the GC effect in the next hadron colliders beyond the LHC energies using these astronomy data. However, we need to consider two problems: (1) the available ZSR equation takes a series of approximations, which may change the predictions of the evolution equation; (2) we can extract E_π^{GC} from cosmic ray spectra, but we do not know which elements construct the target A in the pA collisions. Thanks to the simplest shape of the GC-solutions, as it is only characterized by a few parameters. All corrections are reflected in these parameters and they can be determined by using the limited experimental data. To be specific, at first, we calculate the A-dependence of (x_c, k_c) and E_π^{GC} using the ZSR equation at the leading order approximation. Next we compare these results with the recorded values of E_π^{GC}. We find that if the parameters are selected appropriately, the solutions of equation (2.1) are roughly consistent with the data of intermediate and heavy nuclei, except there are big differences in light nuclei. Then, we look for the reasons and improve the predictions. The results are used to discuss the GC-threshold in the LHC energy range, We find that the interaction energies in the $p-Pb$ and $Pb-Pb$ collisions at the LHC are close to the GC-energy region. Note that the cross section of pion production in the hadronic colliders can be increased by several orders of magnitude due to the GC effect, and about half of the proton kinetic energy converted to the photons of energy $E_\gamma = m_\pi/2$ with an extra intensity in a narrow space at the moment of collision [4]. Therefore, we issue a warning for the next accelerator plans since such unexpectedly intense gamma-rays in the laboratory may damage the detectors.

The organization of the paper are as follows. We give a brief review of the GC solution and nuclear dependent GC effect in cosmic gamma-ray spectra in sections 2 and 3, respectively. The discussions of the GC effect in the LHC and the conclusions are given

in last section.

2 The GC-solutions in nuclei

The unintegrated gluon distribution $F(x,k_T^2)$ of a bound nucleon in the nucleus A (A is the mass number of a nucleus or a complex element) satisfies the following evolution equation, which is derived at the leading logarithmic ($LL(1/x)$) approximation in [2,3]

$$\begin{aligned}
&-x\frac{\partial F(x,k_T^2)}{\partial x} \\
&\simeq \frac{3\alpha_s k_T^2}{\pi}\int_{k_{T,min}^2}^{\infty}\frac{dk_T'^2}{k_T'^2}\left\{\frac{F(x,k_T'^2)-F(x,k_T^2)}{|k_T'^2-k_T^2|}+\frac{F(x,k_T^2)}{\sqrt{k_T^4+4k_T'^4}}\right\} \\
&-\frac{81}{16}\frac{\alpha_s^2 A^{1/3}}{\pi R_N^2}\int_{k_{T,min}^2}^{\infty}\frac{dk_T'^2}{k_T'^2}\left\{\frac{k_T^2F^2(x,k_T'^2)-k_T'^2F^2(x,k_T^2)}{k_T'^2|k_T'^2-k_T^2|}+\frac{F^2(x,k_T^2)}{\sqrt{k_T^4+4k_T'^4}}\right\}. \qquad (2.1)
\end{aligned}$$

This equation keeps the singular structures both in the linear and nonlinear kernels, which correspond to the random evolution of gluons in the k_T-space, where $k_T^2-k_T'^2$ may cross over zero. Note that these infrared divergences have been regularized by the TOPT cutting rule [11].

The evolution of the BFKL dynamics may become nonperturbative near the singular range mentioned above. Fortunately, either the QCD lattice simulations or the nonperturbative dynamics of QCD show that the effective strong coupling constant is restricted by $\alpha_s/\pi \leq B$, B is a constant [12]. For simplicity, we take a fixed value $\alpha_s \equiv 0.3$ in this work.

We take a simple parameterized gluon saturation distribution proposed by Kharzeev-Levin (k-L model) as the input for equation (2.1) at x_A [13]

$$F(x_A,k_T^2)=\begin{cases} f_0 k_T^2 & if\ k_T^2 \leq Q_{A,s}^2 \\ f_0 Q_{A,s}^2 & if\ k_T^2 > Q_{A,s}^2 \end{cases}, \qquad (2.2)$$

where $Q_{A,s}^2=Q_s^2A^{1/3}$, $Q_s=1\ GeV$ is the saturation scale of a free nucleon [14].

Generally, the bigger the nucleus, the earlier the equation (2.1) works. The GC-effect originates from the chaotic solution of equation (2.1). Once a most robust chaos is created, it will dominate the whole process of the condensation, no matter the event occurs whether in the longitudinal ($\sim A^{1/3}$) or horizontal ($\sim A^{2/3}$) area of the nucleus [4]. We call it the GC-uniqueness. Therefore, the starting point of evolution in equation (2.1) is proportional to the volume of a nucleus rather than its longitudinal scale, i.e., we take $x_A = x_p A$, x_p is the starting point of the evolution (2.1) in a free nucleon.

A schematic solution of equation (2.1) is presented in figure 1, which shows the evolution from the CGC distribution at (x_A, Q_s^2) to the gluon condensate at (x_c, k_c^2). One can find that the GC is characterized by a δ function-like form at (x_c, k_c). We use the input equation (2.2) and $x_p \equiv 1.9 \times 10^{-8}$ to calculate the relation $(x_c, k_c) \sim A$. The results are drawn in figures 2 and 3. We will compare them with the cosmic gamma-ray spectra in the following sections.

3 Nuclear dependent GC effect in cosmic gamma-ray spectra

According to the hadronic model, the VHE gamma-ray emissions are dominated by neutral pion decay in the cascade process: $p + p \to \pi^0 + others$ and $\pi^0 \to 2\gamma$. In this process about half energy of the parent protons is taken away by the valence quarks, forming the leading particles, and the remaining energy is transformed into the secondary hadrons (mainly pions) in the central region through gluons→quark-antiquark pairs.

In general, the more the gluons, the more the secondary pions. The GC effect squeezes a large number of gluons with less than x_c to the GC-critical point x_c, so that the number of pions at the GC-threshold E_π^{GC} corresponding to x_c is suddenly increased and reaches a maximum pion yield. As an extreme consideration, we assume that almost all the available kinetic energies of collisions at the center-of-mass system are used to create pions. Taking

this approximation, we can avoid the complicated hadronization mechanism. Combining with the relativistic invariance and energy conservation, one can straightforwardly obtain the following relations [5,6]

$$\ln N_\pi = 0.5 \ln E_{pp} + a, \quad \ln N_\pi = \ln E_\pi + b, \tag{3.1}$$

where $E_\pi \in [E_\pi^{GC}, E_\pi^{max}]$, $a \equiv 0.5\ln(2m_p) - \ln m_\pi + \ln K$ and $b \equiv \ln(2m_p) - 2\ln m_\pi + \ln K$. $K \simeq 1/2$ is inelasticity. Equation (3.1) gives the following special relation

$$E_{pp} = e^{-2(a-b)} E_\pi^2 = \frac{2m_p}{m_\pi^2} E_\pi^2, \tag{3.2}$$

Substituting (3.1) and the standard spectrum of $\pi^0 \to 2\gamma$ into the flux of high energy gamma-rays

$$\Phi_\gamma(E) = C_\gamma \left(\frac{E}{1GeV}\right)^{-\beta_\gamma} \int_{E_\pi^{min}}^{E_\pi^{max}} dE_\pi \left(\frac{E_{pp}}{1GeV}\right)^{-\beta_p} N_\pi(E_{pp}, E_\pi) \frac{d\omega_{\pi-\gamma}(E_\pi, E)}{dE}, \tag{3.3}$$

one can get the GC-characteristic spectrum

$$E_\gamma^2 \Phi_\gamma^{GC}(E_\gamma) \simeq \begin{cases} \frac{2e^b C_\gamma}{2\beta_p - 1} (E_\pi^{GC})^3 \left(\frac{E_\gamma}{E_\pi^{GC}}\right)^{-\beta_\gamma + 2} \\ \qquad\qquad \text{if } E_\gamma \le E_\pi^{GC}, \\ \frac{2e^b C_\gamma}{2\beta_p - 1} (E_\pi^{GC})^3 \left(\frac{E_\gamma}{E_\pi^{GC}}\right)^{-\beta_\gamma - 2\beta_p + 3} \\ \qquad\qquad \text{if } E_\pi^{GC} < E_\gamma < E_\pi^{cut}, \\ \frac{2e^b C_\gamma}{2\beta_p - 1} (E_\pi^{GC})^3 \left(\frac{E_\gamma}{E_\pi^{GC}}\right)^{-\beta_\gamma - 2\beta_p + 3} \exp\left(-\frac{E_\gamma}{E_\pi^{cut}} + 1\right). \\ \qquad\qquad \text{if } E_\gamma \ge E_\pi^{cut}, \end{cases} \tag{3.4}$$

where the lower limit E_π^{min} of integral in (3.3) is E_π^{GC} (or E_γ) if $E_\gamma \le E_\pi^{GC}$ (or $E_\gamma > E_\pi^{GC}$). The upper limit $E_\pi^{max} = 14(E_\pi^{GC})^2$ (in the GeV-unit) if the charged particles can be accelerated continuously [4,5]. However the actual E_π cannot reach such high limit because the restriction of acceleration mechanism. Therefore, we use a smaller cut energy E_π^{cut} to replace E_π^{max}. E_π^{cut} relates to the accelerator mechanism and $E_\pi^{cut} \gg E_\pi^{GC}$ since equation

(3.3) needs a sufficiently wide integration interval. According to the numerical simulation, E_π^{cut} is required at least one order of magnitude greater than E_π^{GC}, i.e., $E_\pi^{cut} \geq 10E_\pi^{GC}$. E_π^{GC} and (x_c, k_c) have the following relation [4,5]

$$E_\pi^{GC} = \exp\left(0.5 \ln \frac{k_c^2}{2m_p x_c} + a - b\right) = \frac{m_\pi}{2m_p} \frac{k_c}{\sqrt{x_c}}. \tag{3.5}$$

Using this equation, one can predict the GC-threshold in figure 4. We find that the distribution of E_π^{GC} can be roughly divided into three ranges: (i) $E_\pi^{GC} \approx 100\ GeV$ for intermediate and heavy nuclei ($A > 100$), (ii) E_π^{GC} quickly increases for light nuclei ($A < 20$) and (iii) the area between them ($20 < A < 100$).

Works [5-10] use the GC-spectrum (3.4) to fit the VHE gamma-ray energy spectra. We summarize some of the GC-thresholds in table 1. Note that $E_\pi^{GC}(p - A) > E_\pi^{GC}(p - A')$ if $A' > A$ since the nonlinear corrections increases with A. Therefore, we consider that the different values of E_π^{GC} arise from the different nuclei. The results are qualitatively consistent with the data, except a big modification is needed in the *pp* and light nuclei collisions. In fact, the Tibet ASγ collaboration reports that gamma-rays from the supernova remnant G106.3+2.7 has a largest recorded GC-threshold $E_\pi^{GC} \simeq 20$ TeV in the galaxy [9,15]. Besides, the hardening VHE gamma-ray spectra in 1ES 1426+428 and (Mkn) 501 imply that the existence of high value of $E_\pi^{GC} \sim 20\ TeV$ in active galactic nuclei (AGN) are possible [8]. Therefore, we suggest that the maximum GC-threshold $E_\pi^{GC} = 20\ TeV$ originates from the *pp* collision ($A = 1$).

To find the reasons of the above deviation for proton and light nuclei, we recheck the approximations in equation (2.1).

(i) The leading order approximation is taken in equation (2.1) and higher order corrections are neglected. We have shown that the high order corrections may product the multi-chaos solution because of the complicated singular structure [4]. In this case, the

solution of the evolution equation is dominated by a most robust chaos and finally forms a single GC solution. Although these corrections may change the relative strength of the nonlinear part of equation (2.1), they are unlikely to product the strong A-dependent value of x_c for light nuclei.

(ii) A possible reason of the strong deviation from $A^{1/3}$-dependence of E_π^{GC} may come from an assumption of the correlation function in equation (2.1). We use a simplified model to explain it.

The two-gluon correlation function $F^{(2)}(x, k_T^2)$ in equation (2.1) is simplified as the square of a gluon distribution, i.e., $F^{(2)}(x, k_T^2) \equiv F^2(x, k_T^2)$. Now let us consider a more general correlation of two different gluon distributions in equation (2.1)

$$F^{(2)}(x, k_T^2) \equiv \int dk_T''^2 R(k_T^2, k_T''^2) F(x, k_T^2) F(x, k_T''^2), \tag{3.6}$$

$R(k_T^2, k_T''^2)$ is a normalized correlation function of two gluons in the nucleon. For simplicity, we take a special correction function, where two gluons are correlated with an equal probability in a given range, i.e.,

$$R(k_T^2, k_T''^2) = \frac{A}{\beta} \theta \left(\frac{\beta}{A} - k_T''^2 + k_T^2 \right), \tag{3.7}$$

where $\theta(z) = 1$ (or 0) if $z \geq 0$ (or $z < 0$). Thus, we have

$$F^{(2)}(x, k_T^2) = F(x, k_T^2) \frac{A}{\beta} \int_{k_T^2}^{k_T^2 + \frac{\beta}{A}} dk_T''^2 F(x, k_T''^2). \tag{3.8}$$

Here we assume that the two correlated gluons in proton or light nuclei are distributed in a broad k_T^2 space, where $\beta/A > Q_{A,s}^2$ ($A < 10$). Using equations (2.2) and (3.8), we have

$$F^{(2)}(x, k_T^2) \equiv F(x, k_T^2) S(x, k_T^2), \tag{3.9}$$

where

$$S(x,k_T^2) = \frac{A}{\beta}\left[\left(k_T^2 + \frac{\beta}{A} - Q_{A,s}^2\right) f_0 Q_{A,s}^2 + \frac{1}{2}(f_0 Q_{A,s}^2 + f_0 k_T^2)(Q_{A,s}^2 - k_T^2)\right]$$
$$= f Q_{A,s}^2 - \frac{1}{2}\frac{A}{\beta} f_0 (Q_{A,s}^2 - k_T^2)^2, \quad if\ k_T^2 < Q_{A,s}^2 \tag{3.10}$$

and

$$S(x,k_T^2) = f_0 Q_{A,s}^2, \quad if\ k_T^2 \geq Q_{A,s}^2. \tag{3.11}$$

Thus, for proton or light nuclei we have

$$F^{(2)}(x,k_T^2) > F^2(x,k_T^2), \quad if\ k_T^2 < Q_{A,s}^2 \tag{3.12}$$

and

$$F^{(2)}(x,k_T^2) = F^2(x,k_T^2), \quad if\ k_T^2 \geq Q_{A,s}^2. \tag{3.13}$$

Note that equation (3.12) uses

$$\Delta S \equiv S - F(x,k_T^2) = f_0(Q_{A,s}^2 - k_T^2)\left[1 - \frac{1}{2}\frac{A}{\beta}(Q_{A,s}^2 - k_T^2)\right]$$
$$> f_0(Q_{A,s}^2 - k_T^2)\left(1 - \frac{1}{2}\frac{A}{\beta}Q_{A,s}^2\right) > f_0(Q_{A,s}^2 - k_T^2)\left(1 - \frac{1}{2}\right) > 0, \tag{3.14}$$

since $\beta/A > Q_{A,s}^2$ in proton.

According to the above analysis, one can find that the slope of $F^{(2)}(x,k_T^2)$ decreases at $k_T^2 \leq Q_{A,s}^2$ comparing with that of $F^2(x,k_T^2)$, which means that the curve $F^{(2)}(x,k_T^2) \sim k_T^2$ becomes flatter than $F^2(x,k_T^2) \sim k_T^2$ at $k_T^2 = Q_{A,s}^2$. As a result, the GC-critical value x_c quickly decreases in proton or light nuclei since a large change of slope of gluon distribution is necessary to create chaos [3,4].

On the other hand, the gluons of different nucleons can penetrate through each other in the infinite momentum frame, the fusion probability of two identical gluons increases

rapidly with the increase of A. Note that once a strong chaos is created, it will dominate the evolution process due to the GC-uniqueness. Thus, the transverse momenta of two correlated gluons are restricted in a narrow interval near k_T^2, i.e., $\beta/A \ll Q_{A,s}^2$. We have

$$S(x,k_T^2) = \frac{1}{2}\frac{A}{\beta}\left[f_0 k_T^2 + f_0\left(k_T^2 + \frac{\beta}{A}\right)\right]\frac{\beta}{A}$$
$$= f_0 k_T^2 + \frac{1}{2}f_0\frac{\beta}{A} \simeq f_0 k_T^2 = F(x,k_T^2), \quad if\ k_T^2 < Q_{A,s}^2. \tag{3.15}$$

Therefore, for heavy nuclei

$$F^{(2)}(x,k_T^2) \simeq F^2(x,k_T^2). \tag{3.16}$$

In fact, in the case of $A/\beta \gg 1$ ($A \gg 100$) in equation (3.7), we have $R(k_T^2, k_T''^2) \to \delta(k_T^2 - k_T''^2)$ and $F^{(2)}(x,k_T^2) \to F^2(x,k_T^2)$. Thus, the GC-critical point x_c in proton or light nuclei is much smaller than that in heavy nuclei.

The above example shows that equation (2.1) is an ideal approximation describing the gluon distributions in heavy nuclei, except the predicted GC-critical value x_c in proton or light nuclei should be reduced due to the corrections of $F^{(2)}(x,k_T^2) \neq F^2(x,k_T^2)$. Considering the complexity of the real correlation function, according to the above results we qualitatively marked out the possible modifications to the solutions of equation (2.1) for the light nuclei in figures 2 and 4.

4 The GC effect in the LHC

The contributions of proton and nucleus in the pA collisions dominate the rapidity distribution on the two sides of rapidity space, respectively. Note that the GC effect begins work when the gluons with x_A takes the first to participate the $A' - A$ collisions if $A > A'$, and enhances the total cross section of the collisions, therefore, we have

$E_\pi^{GC}(p-A) \simeq E_\pi^{GC}(A-A)$, although the GC-signal strength of the former is half weaker than the latter.

The upper limit of integral in equation (3.3) will be fixed by a maximum energy of the collider. As we have known, the GC effect causes a big excess in the cross section of hadron collisions at center-of-mass energy $\sqrt{s^{GC}}$. In table 2 we give these thresholds using equations (3.2), (3.5) and the modified curve in figure 4. For example, we take $E_\pi^{GC}(p-p) = 20$ TeV, thus, $E_{pp}^{GC} = 100 \times (2 \times 10^4)^2$ GeV$= 4 \times 10^{10}$ GeV and $\sqrt{s_{pp}^{GC}} = \sqrt{2m_p E_{pp}^{GC}} = 3 \times 10^2$ TeV. Note that E_π^{GC} is a lower integral limit in equation (3.3). To observe the GC effect in the pp collision, one needs $E_\pi^{cut} \geq 10 E_\pi^{GC}$, which requires $\sqrt{s_{pp}^{cut}} \geq 3 \times 10^3$ TeV. The maximum energies of the pp collision at the LHC is $\sqrt{s_{pp}} = 13$ TeV $\ll 3 \times 10^3$ TeV. Obviously, we can not record any GC-signals from the pp collision in the recent LHC.

Now we consider the $p-Pb$ and $Pb-Pb$ collisions at the LHC, their maximum energies are 8.16 TeV and 5.02 TeV, respectively. Referring to figure 4, we take $E_\pi^{GC}(Pb-Pb) =$ 100 GeV for them. The results are presented in table 2. The energy region where the GC-signal appears is $\sqrt{s_{pPb}^{cut}} > 10$ TeV. Although the energies of these collisions in the LHC are already close to the GC-thresholds, it is still necessary to further increase the collision energy.

We emphasize that the GC effect may efficiently convert the kinetic energy of the parent protons into a large number of secondary particles. In fact, the multiplicity of mini gluon-jets in the hadronic collisions with the GC effect is about $10^3 - 10^4$ times larger than that without the GC model [4]. Besides, there is a highest gluon-pion conversion rate in the GC model. Thus, about half of the kinetic energy of protons are converted to the large numbers of photons with energy $E_\gamma = m_\pi/2$ in the center of mass (CM) frame in the $Pb-Pb$ collision. Such monochrome gamma rays have extra high strength in a

narrow space, and may damage the detectors in the laboratory.

We noticed that the Auger collaboration indirectly used the cosmic ray data at the top of the atmosphere and found that pA cross section at $\sqrt{s} \sim 100\ TeV$ is the normal value $\sim 567\ mb$ with no big increment [16]. According to figure 4 we guess that the GC-threshold $E_{\pi}^{GC}(p-atm) > 1\ TeV$ for light nuclei at the top of atmosphere. which implies $\sqrt{s_{p-atm}^{GC}} > 10\ TeV$, and $\sqrt{s_{p-atm}^{cut}} > 100\ TeV$. This result means that the observed energy by Auger collaboration at $\sqrt{s} = 100\ TeV$ is close to the lower-limit of the GC-effect range if the above mentioned indirect estimations are correct.

The more direct method of probing the GC effect in the laboratory is the Electron Ion Collider (EIC) [17] and the Large Hadron electron Collider (LHeC) [18]. The designed collision energy of upcoming EIC(US) is $\sqrt{s_{eA}} \simeq 140\ GeV$, which is in the CGC range $(x > 10^{-5}, Q^2 > 1\ GeV^2)$. According to our estimation in figure 2, the range of the GC effect is $(x_c \simeq 10^{-6}, k_c^2 \simeq 5\ GeV^2)$, which exceeds the range of the EIC(US). However, the center-of-mass energy of the proposed Large Hadron electron Collider (LHeC) $\sqrt{s_{eA}} \sim 1$ TeV will be able to cover a very low x-range: $x \sim 10^{-6}$ at $Q^2 > 1GeV^2$ in eA collisions, where we may record the GC-signal.

Conclusions: We find that the hadron collisions $p - Pb$ and $Pb - Pb$ in the LHC are already close to the energy region of the GC effect. Since the huge number of gluons are condensed in a critical momentum (x_c, k_c), it should greatly increase the hadron cross section and release strong gamma-rays. We warn that further increase of the hadron collision energies in the next LHC plans will lead to unexpectedly intense gamma rays in the accelerator, they like the artificial mini GRBs and may damage the detectors

Acknowledgments: We thank K. Murugan for useful comments. This work is supported by the National Natural Science of China (No.11851303).

References

[1] L. McLerran, *The CGC and the glasma: Two Lectures at the Yukawa Insitute,* [arXiv:1011.3204].

[2] W. Zhu, Z.Q. Shen and J.H. Ruan, *Can a chaotic solution in the QCD evolution equation restrain high-energy collider physics? Chin. Phys. Lett.* **25** (2008) 3605 [arXiv:0809.0609].

[3] W. Zhu, Z.Q. Shen and J.H. Ruan, *The chaotic effects in a nonlinear QCD evolution equation, Nucl. Phys.* **B911** (2016) 1 [arViv:1603.04158]

[4] W. Zhu and J. Lan, *The gluon condensation at high energy hadron collisions, Nucl. Phys.* **B916** (2017) 647 [arXiv:1702.02249].

[5] W. Zhu, J.S. Lan and J.H. Ruan, *The gluon condensation in high energy cosmic rays, Int. J. Mod. Physics* **E27** (2018) 1850073 [arXiv:1709.03897].

[6] F. Feng, J.H. Ruan, F. Wang and W. Zhu, *Looking for the Gluon condensation signature in protons using the Earth-limb gamma-ray spectra. Astrophys. J.* **868** (2018) 2.

[7] W. Zhu, P. Liu, J.H. Ruan and F. Wang, *Possible evidence for the gluon condensation effect in cosmic positron and gamma- ray spectra. Astrophys J* **889** (2020) 127.

[8] W. Zhu, Z.C. Zheng, P. Liu, L.H. Wan, J.H. Ruan and F. Wang, *Looking for the possible gluon condensation signature in sub-TeV gamma-ray spectra: from active galactic nuclei to gamma ray bursts, JCAP.* **01** (2021) 038[arXiv:2009.01984].

[9] J.H. Ruan, Z.C. Zheng and W. Zhu, *Exploring the possible gluon condensation signature in gamma-ray emission frompulsars, JCAP* 08 (2021) 065.

[10] W. Zhu, P. Liu and Z.Y. Cui, *The gluon condensation in the proton as an origin of ultrahigh-energy γ-rays in the galaxy.* (2021) [arXiv:].

[11] W. Zhu, *A new approach to parton recombination in the QCD evolution equations, Nucl. Phys.* **B551** (1999) 245.

[12] C. D. Roberts, *Insights into the origin of mass,* [arXiv:1909.12832].

[13] D. Kharzeev and E. Liven, *Manifestations of high density QCD in the first RHIC data, Phys. Lett.* , **B523** (2001) 79.

[14] Y.V. Kovchegov and E. Levin,*Quantum chromodynamics at high energy,* (2012) Cambridge university press.

[15] M. Amenomori, Y.W. Bao and X.J. Bi et al., *Potential PeVatron supernova remnant G106.3+2.7 seen in the highest-energy gamma rays. Nature Astron.* (2021) doi:10.1038/s41550-020-01294-9.

[16] R. U. Abbasi, M. Abe, T. Abu-Zayyad, *Measurement of the proton-air cross section with telescope array's middle drum detector and surface array in hybrid mode Phys. Rev.* **D92** (2015) 032007.

[17] R. Abdul Khalek, A. Accardi and J. Adam, et al., *Science Requirements and Detector Concepts for the Electron-Ion Collider, (EIC Yellow Report)* (2021) BNL-220990-2021-FORE, JLAB-PHY-21-3198, LA-UR-21-20953.

[18] P. Agostini1, H. Aksakal and S. Alekhin, et al., (LHeC and FCC-he Study Group) *The Large Hadron-Electron Collider at the HL-LHC,* (2020) [arXiv:2007.14491].

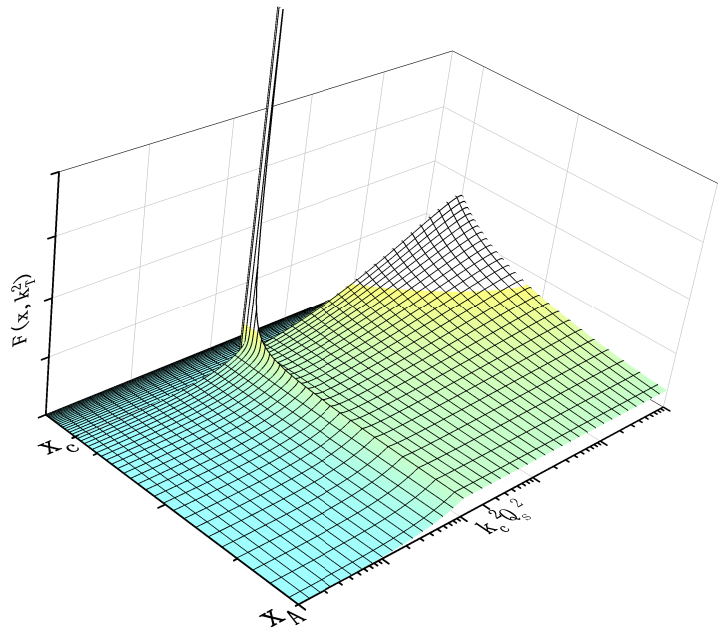

Figure 1: A schematic diagram for the evolution of gluon distribution in equation (2.1) from the CGC at (x_A, Q_s^2) to the GC at (x_c, k_c^2).

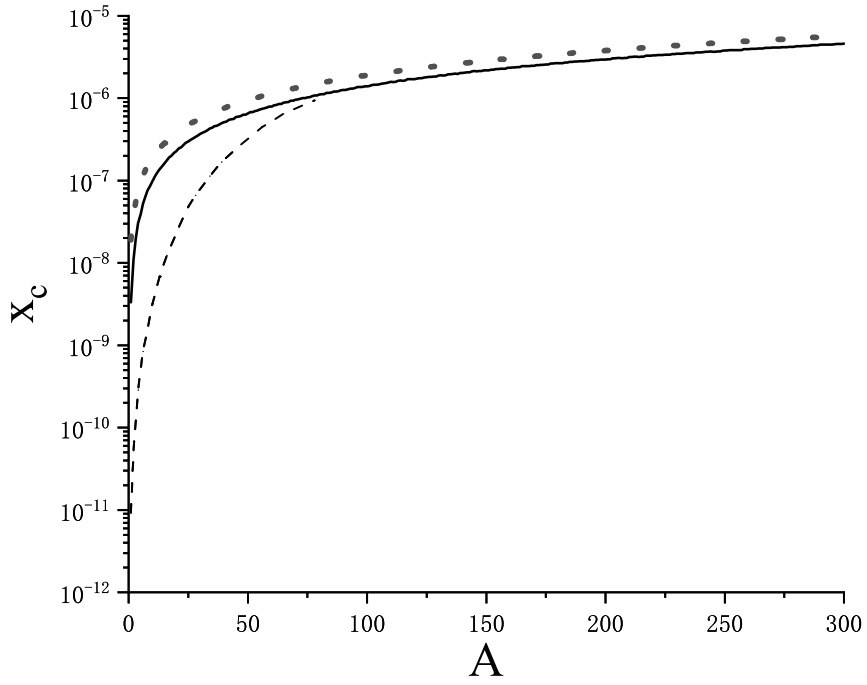

Figure 2: Predicted critic momentum x_c (solid curve) in different nuclear target. The point curve is $x_A = 1.9 \times 10^{-8} A$. The dashed curve is the possible modified x_c due to equation (3.6).

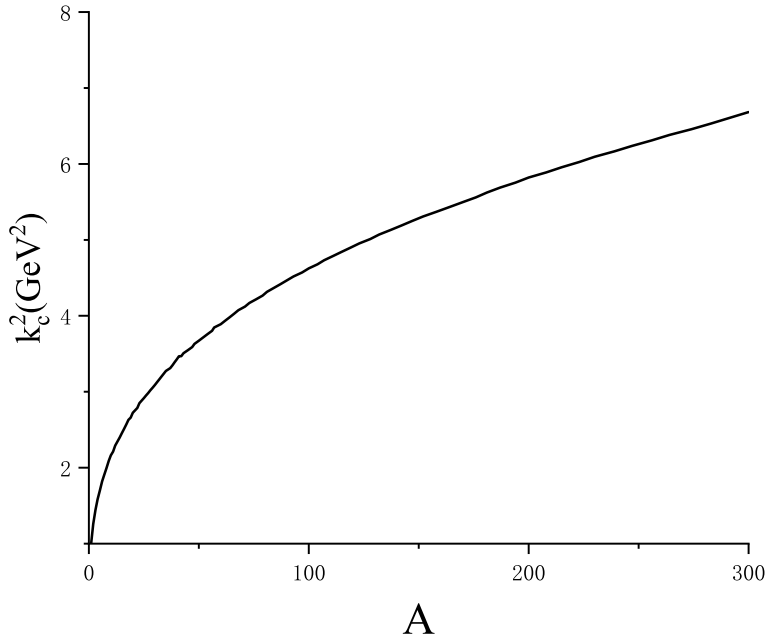

Figure 3: Predicted critic momentum k_c^2 in different nuclear targets.

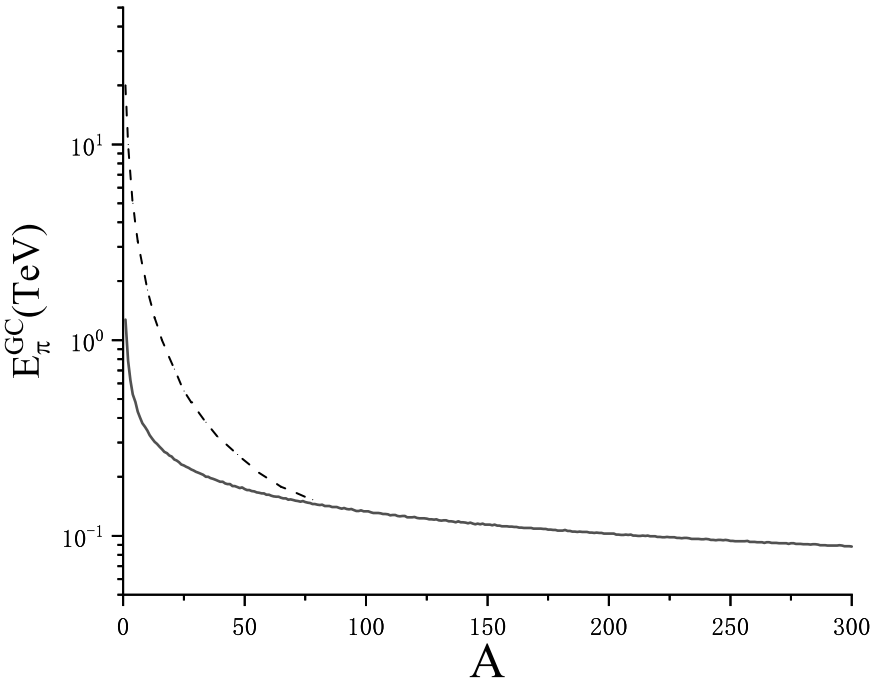

Figure 4: The predicted GC-threshold E_π^{GC} in pA (or $A-A$) collisions (solid curve), which are obtained by equation (3.5) and the data of figures 2 and 3. The dashed curve is the possible modified GC-threshold E_π^{GC} due to equation (3.6).

Table 1: The GC-thresholds E_{π}^{GC} extracted from different gamma-ray spectra.

Spectrum	$E_{\pi}^{GC}(GeV)$	Ref.
G106.3+2.7	2×10^4	[10]
H1426+428	10^4, 3×10^2	[8]
LES0229+202	3×10^3, 3×10^2	[8]
Tycho	4×10^2	[7]
PKS2155-304	1.4×10^2	[8]
LES1959+650	1.3×10^2	[8]
H2356-309	10^2	[8]
PG1553+113	10^2	[8]
J1641-463	10^2	[9]
3C58	10^2	[9]

Table 2: Predicted the center-of-mass energy $\sqrt{s_{pA}^{cut}}$ appearing the GC effect and relating quantities in different hadronic collisions (in the GeV-unit).

Collisions	E_{π}^{GC}	E_{pA}^{GC}	$\sqrt{S_{pA}^{GC}}$	E_{π}^{cut}	E_{pA}^{cut}	$\sqrt{S_{pA}^{cut}}$
p-p	2×10^4	4×10^{10}	3×10^5	2×10^5	4×10^{12}	3×10^6
p-atm	$> 10^3$	$> 10^8$	$> 10^4$	$> 10^4$	$> 10^{10}$	$> 10^5$
p-Pb or Pb-Pb	10^2	10^6	10^3	10^3	10^8	10^4